Construction and Building Materials 472 (2025) 140881

Contents lists available at ScienceDirect

Construction and Building Materials

journal homepage: www.elsevier.com/locate/conbuildmat

Mortar-mini -vascular networks filled with nanolimes: An innovative biomimetic approach for enhancing resilience in built heritage

C. De Nardi [a,*], R. Giorgi [b]

[a] Resilient Structures and Construction Materials (RESCOM) Research Group, School of Engineering, Cardiff University, Queen's Buildings, The Parade, Cardiff, Wales CF243AA, United Kingdom

[b] Consorzio per lo Sviluppo dei Sistemi a Grande Interfase (CSGI), University of Florence, Via Della Lastruccia 3, Sesto Fiorentino 50019, Italy

ARTICLE INFO

Keywords:
Self-healing
Lime-based mortars
Built heritage

ABSTRACT

Climate change is increasingly exposing our built heritage to a wider range of extreme hazards. In response to these challenges, it is crucial for historic masonry repair technologies to adapt and promote a resilient preservation strategy that can withstand long-term impacts. Inspired by biomimetic technologies, this research introduces the use of 4D-printed mortar-mini vascular networks (m-MVNs) for repairing cracks in lime-based mortars. m-MVNs consist of interconnected channels- made from polylactide acid (PLA) – designed to fit completely within the mortar joint. The study explored the properties of tailored nanolime dispersions as healing agents. Two different blends were studied with varying alcohol/water ratios, specifically 10 g/L of calcium hydroxide in either a 50:50 or 80:20 water:ethanol mixture. Specimens were pre-cracked at different ages (28–196 days) and three levels of damage (70 % of the compression strength in pre-peak regime; 90 % of the compression strength in post and pre-peak regime) and then healed for 14 days. Some self-healing ability was observed in the plain lime samples, with enhanced performance in samples containing empty m-MVNs. m-MVNs filled with nanolime demonstrated strong healing performance, with the 50:50 dispersion being the most promising, achieving a ceiling healing index of 37 % in strength and 53 % in stiffness.

1. Introduction

Across centuries, architectural heritage has been built using masonry, clay, stone elements, and lime-based mortars. As time passes, environmental factors subject these structures to gradual deterioration, resulting in microcracks that can compromise their integrity.

In recent years, lime-based materials have garnered significant attention for their applications in the restoration and conservation of cultural heritage buildings [1–5]. This renewed interest stems from lime's compatibility with historical materials and its intrinsic healing properties, which position it as a sustainable and environmentally friendly alternative to cement-based solutions [6].

One of the most compelling properties of lime-based mortars is their capacity for autogenous healing, a phenomenon where materials repair cracks and partially restore mechanical properties under specific conditions [7]. This process involves water dissolving calcium-bearing compounds and transporting them from binder-rich areas to voids and cracks within the mortar. As the dissolved compounds re-crystallize, they effectively seal the cracks, contributing to the material's ability to self-heal and enhance its durability [8]. This mechanism helps to mitigate the progression of damage and ensuring the longevity of heritage structures [9].

Several studies have explored the factors influencing autogenous healing in lime mortars [10,11] Garijo et al. [12] demonstrated that loading frequency in natural hydraulic mortars significantly enhances their residual strength through the rehydration of unreacted components under cyclic loads. Similarly, De Nardi et al. [13] highlighted that the timing of pre-cracking significantly affects the strength recovery, with earlier pre-cracking yielding better outcomes. These findings underscore the need for innovative approaches to extend the healing capacity of lime mortars over time.

Recent advancements have focused on enhancing the performance of lime-based mortars through the incorporation of smart additives [14] and nanomaterials [15]. Santhanam et al. [16] investigated the effects of carboxymethyl cellulose (CMC) and alccofine (AF) on the hydraulic and durability properties of natural hydraulic lime mortars, revealing improved freeze–thaw resistance with a long healing period. Moreover, Vucetic et al. [17] examined the surface healing of original medieval

* Corresponding author.
E-mail addresses: denardic@cardiff.ac.uk (C. De Nardi), rodorico.giorgi@unifi.it (R. Giorgi).

https://doi.org/10.1016/j.conbuildmat.2025.140881
Received 18 November 2024; Received in revised form 11 March 2025; Accepted 13 March 2025
Available online 25 March 2025

mortars from Bač Fortress, Serbia, and laboratory-replicated mortars using a two-component bacterial system (*Sporosarcina pasteurii DSM 33* and nutrients). Healing efficiency was lower in the original mortars, likely due to insufficient free calcium ions needed for the reactions [18].

The study of self-healing in cement-based materials is a field that has developed extensively over the last decades [19,20,21], exploring the use of microcapsules [22–24] vascular networks [25–27], additives [28–31] to extend the service life of the material and thus reducing long-term costs of maintenance.

Building upon these innovations, researchers at Cardiff University proposed the concept of mini-vascular networks (MVNs) as an alternative approach to continuous vascular networks for self-healing concrete structures. MVNs are 3D-printed units with interconnected channels that mimic the arterial system of the human body (biomimicry). They can store and protect healing agents, which are released when threshold damage is exceeded.

De Nardi et al. [32,33] further developed this concept by designing tetrahedral-shaped microvascular networks (MVNs), known as TETs or d-TETs which can be seamlessly incorporated into wet concrete during the mixing process. These MVNs are capable of storing healing agents, either single- or bi-component, within concrete prisms. In samples embedding TETs filled with sodium silicate (SS), notable recoveries of 20 % in strength and 75–80 % in stiffness were achieved [30]. Additionally, samples containing d-TETs filled with SS in combination with either nanolime (Nlime) or nanosilica (Nsilica) solutions demonstrated an extra 10 % increase in recovery [33].

This work introduces a concept that MVNs is a flexible system that allow the transfer from newly constructed concrete structures design to the restoration of historical masonry walls. The size and configuration of previous MVNs have been completely re-evaluated, resulting in the development of mortar-mini vascular networks (m-MVNs) that can be positioned entirely within the thickness of the mortar joints.

In traditional restoration practices, when extensive masonry deterioration causes mortar joints to lose their functionality, patching techniques are employed to restore structural integrity while preserving the original blocks [34,35]. These techniques involve retaining the original stones or bricks while renewing the mortar joints. In this context, m-MVNs can be integrated into the new mortar joints during the reworking process, allowing their installation to coincide seamlessly with the restoration work.

This paper evaluates the physico-chemical and mechanical compatibility of m-MVNs with hydraulic lime mortar, as well as their efficiency in storing and delivering nanolime dispersions. Furthermore, tailored nanolime dispersions are developed and analysed, ensuring their suitability for this self-healing technology (as described in Section 2.2).

The use of calcium hydroxide in the building industry and Cultural Heritage conservation is well-established, relying on the well-known carbonation reaction and the properties of the calcium carbonate (CaCO3) that forms [36–38].

In 2001, Giorgi et al. [39] firstly developed and tested nanoparticles of calcium hydroxide, known as nanolimes, for the treatment of wall-paintings. This innovative approach effectively overcame the limitations associated with the traditional limewater treatment, which showed low consolidation capacity due to limited solubility in water and high diffusion and spreading in large volume through capillarity [40]. Nanolimes are colloidal alcoholic or hydro-alcoholic dispersions characterised by increased quantity of lime particles and reduced size, which increases their reactivity and concentration [41,42]. When applied to mortar for repair, the aforementioned attributes contributed to an enhanced and durable consolidating effect when compared to conventional consolidants [43,44]. The main advantage relies on the physico-chemical compatibility when used on carbonate-based stones or mortars. The formation of crystalline carbonate confers higher mechanical properties, preserving the original materials from unpredictable side-processes, which usually occur at the interface with consolidants whose composition differs significantly both in chemical and mineralogical terms. Recently, the carbonation kinetics $Ca(OH)_2$ nanoparticles' dispersions was investigated by Camerini et al. [45]. The authors used four types of $Ca(OH)_2$ nanoparticle dispersions in humid air and found that during carbonation, the boundary regions of the particles densely populated with $CaCO_3$ nuclei undergo early transformation, followed by thickening of slab-like regions around the original boundaries [45].

The aim of this paper is to: (i) evaluate the compatibility of m-MVNs with lime-based mortars through compression tests, (ii) assess their effectiveness as carriers for nanolime, and (iii) examine the healing efficiency of the system.

Cubic specimens were subjected to compression tests until failure or pre-cracked at various damage levels in both the pre-peak and post-peak regimes. Nanolime dispersions with varying water-to-ethanol ratios were prepared to minimize potential negative interactions with the PLA polymer while enhancing healing efficiency.

Section 2 provides an overview of the m-MVNs design concept and its application in masonry structures, alongside descriptions and analyses of the nanolime dispersions used in the study. Section 3 details the experimental program, including the setup for uniaxial compression tests. The subsequent section presents the experimental results and discussion, covering the evaluation of mechanical properties and healing efficiencies observed in specimens containing m-MVNs, as well as SEM analyses to examine the characteristics of the hardened healing products.

2. Materials and methods

2.1. m-MVNs design

Research conducted at Cardiff University has demonstrated that 3D printed MVNs effectively overcome the issue of suction that arises in 1D tubular capsules, which hinders the proper release of liquid healing agents [32]. Digital microscopy conducted on tetrahedral shape MVNs showed strong inter-layer adhesion between the layers led to the creation of impermeable units.

The surface profile of the MVNs created via 3D printing, in conjunction with the rib design, resulted in a textured surface that promoted a strong bond with the cementitious matrix. Throughout the testing program, no instances of MVN debonding were observed, thus ensuring that the channels fractured when subjected to concrete cracks of serviceable size [33].

Building upon the findings of earlier studies conducted on single or dual-channel MVNs, the criteria for manufacturing m-MVNs to restore historic masonry structures are as follows: i) capable of being fully accommodated within the thickness of mortar joints (10–15 mm); ii) capable of rupturing at the designed crack opening value; iii) entirely watertight, effectively preventing any chemical interactions between the healing agents and the lime matrix prior to breakage; iv) employing a 4D printing process that is both easily repeatable and functional.

The concept of 4D printing relies on the ability of the system to respond dynamically to external stresses. These stresses act as external stimuli, triggering the rupture and subsequent controlled release of the healing agent precisely when and where it is needed, thereby enhancing the self-healing efficiency of the system. Several preliminary investigations were undertaken to establish a successful and convenient 4D printing process that could be repeated consistently for manufacturing m-MVNs, details on the optimisation and printing process can be found in De Nardi et al. [46].

m-MVNs were manufactured by using Verbatim transparent PLA filament with a diameter of 2.85 mm. The printing process was carried out using an Ultimaker2$^+$® printer (Utrecht, Netherlands) equipped with a 0.25 mm nozzle and a layer height of 0.06 mm.

m-MVNs were formed with a grid scaffold structure to optimise the properties of the unit as a function of the printing orientation. The print speed was set at 60 mm/sec and printing temperature at 185 °C. To

improve the adhesion of the printed m-MVNs to the build platform, a brim with a length of 250 mm and a height of 8 mm was used. Initial layer height and infill line width was kept equal to 0.25 mm. To enhance printing accuracy and achieve full watertightness, adaptive slicing algorithms were employed, dynamically adjusting the layer thickness with a tolerance of 0.02 mm, based on the geometric characteristics of the model.

The most successful version on MVNs is represented in Fig. 1.

Fig 2 depicts printed m-MVNs, showing both empty and ink-filled versions. The figure provides visual evidence of their complete watertight integrity, as demonstrated by the absence of ink leakage when submerged in water.

Approximately 2 mL of nanolime dispersions were injected into each m-MVN using a syringe through a pre-drilled hole at the top of the ligament, which was then sealed with silicone.

2.2. Healing agent selection

The effectiveness of the m-MVN technology relies on the key healing principle, which involves the timely rupture of the m-MVN channels, followed by the flow of healing agents into the crack location, and sufficient curing time for the healing agent. The selection of the healing agents has prioritised compatibility criteria, ensuring that the active healing agents are physically, chemically, and mechanically compatible with the host materials to meet conservation requirements.

Considering the narrow dimensions of the channels and the designed crack width of 0.05–0.1 mm, low-viscosity healing agents were the chosen preference. This choice aims to facilitate the filling process of the m-MVNs and ensure the efficient release of healing agents upon crack occurrence. Additionally, the low viscosity of these agents promotes effective penetration and uniform dispersion within the lime matrix.

As described in the previous section, nanolimes have been extensively used in the preservation of wall paintings, limestones, and stuccoes, wherein they have successfully achieved the re-adhesion of detached particles or pigment flakes [47].

Previous studies that focused on 3D-printed PLA tetrahedral MVNs filled with a nanolime ($Ca(OH)_2$) alcohol suspension, specifically Nanorestore® produced by CSGI - University of Florence and marketed by the company CTS Europe, have indicated that the adsorption of these agents onto the polymer surface, in combination with exposure to an alkaline environment, can potentially impact the physical properties of the material. [33]. Differential Scanning Calorimetry (DSC) measurements have shown that the presence of isopropyl alcohol in the nanolime dispersion could lead to transesterification reactions. These reactions may have further contributed to the degradation of the material [33].

Moreover, recent studies have demonstrated that the deposition of nanolime can be controlled by adjusting its properties, such as kinetic stability and evaporation rate, to match the moisture transport characteristics of the substrate [48].

In this research, the nanolime dispersions have been further optimized for their application in m-MVNs systems. To overcome potential degradation of the PLA polymer, efforts were made to reduce the volume of alcohol while ensuring that the blend remained stable and that clustering of nanoparticles did not lead to particles packing, allowing an

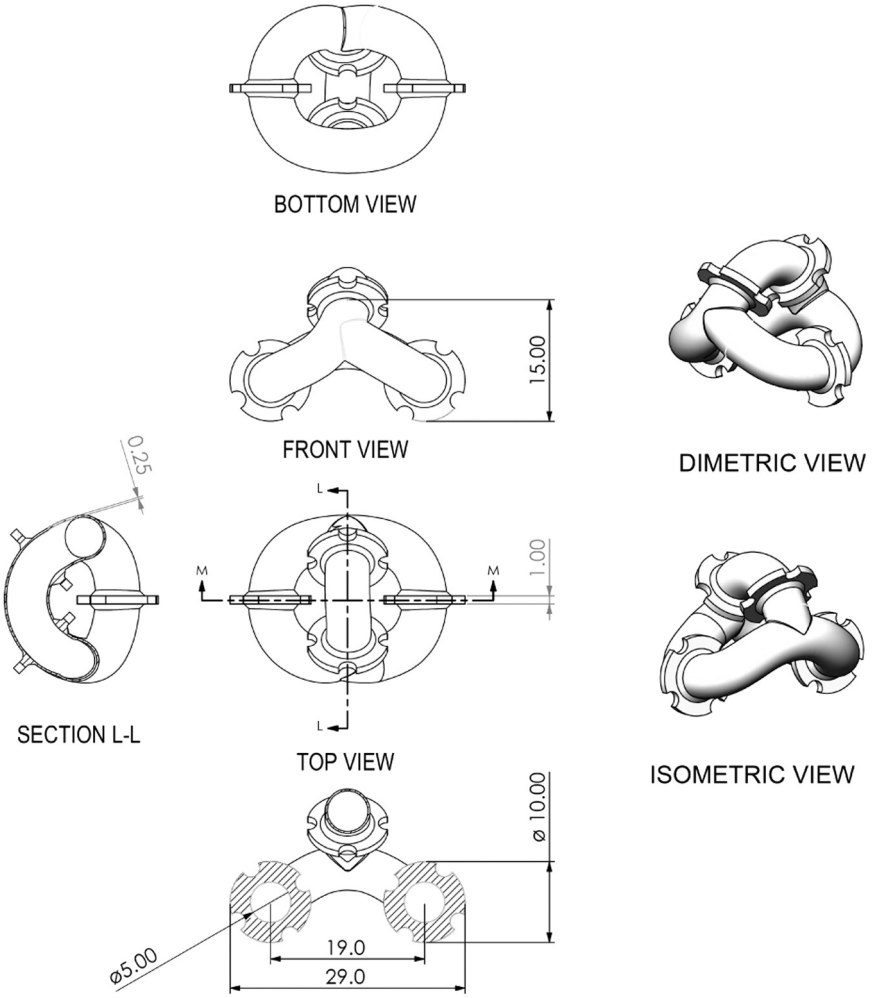

Fig. 1. Dimensions of a m-MVN unit (dimensions in mm).

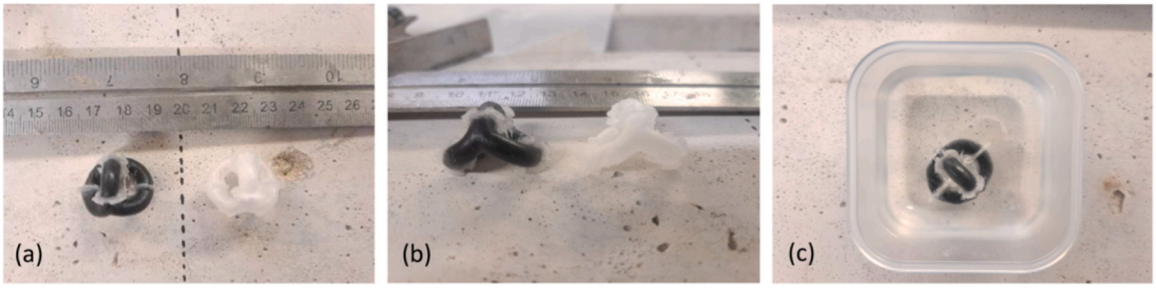

Fig. 2. 4D printed m-MVNs empty and filled with ink, top view (a); front view (b); full watertight (c).

effortless redispersion of nanoparticles.

Two nanolime dispersions were evaluated, namely 50:50 = 10 g/L calcium hydroxide in 50–50 % water – ethanol and 80: 20 = 10 g/L calcium hydroxide in 80–20 % water – ethanol.

2.3. Mix details

NHL (Natural Hydraulic Lime) of class HL3.5 according to EN 459–1 [49], supplied by "Tarmac," was used to prepare the mortars. The fine aggregate sand employed was 0–2 mm, following BS EN 13139–2013 [50]. The binder/sand ratio and the water/lime ratio were maintained at 1:3 by weight and 1:0.7 respectively, as commonly used for historical mortars [51–53]

The same mix proportions, constituents and mixing protocol were used throughout the experimental programme. The dry materials (lime and sand) were mixed for 120 s, at which point the water was introduced whilst the mixer was rotating.

As can be seen in Fig 3, 100 mm× 100 mm x100 mm moulds were filled in 3 layers and vibrated for 60 s each layer to a maximum of 45 Hz. In the middle layer, five m-MVNs were manually placed. Four of these m-MVNs were positioned at the corners of the cube, while the remaining one was placed in the centre.

Samples were kept in the moulds covered with a damp Hessian sheet for seven days. After this, the samples were demoulded and stored in a sealed container covered with a damp Hessian cloth to provide high relative humidity values (>90 %, 20° C ± 5°) up to the first test, i.e. 28 days or 168 days.

2.4. Experimental arrangement and programme

All specimens were loaded under displacement control, at a rate 0.3 mm/min using a MATEST/C091–02N machine equipped with a Servo-plus progress control unit. The three-stage testing procedure is as follows, as represented in Fig. 4:

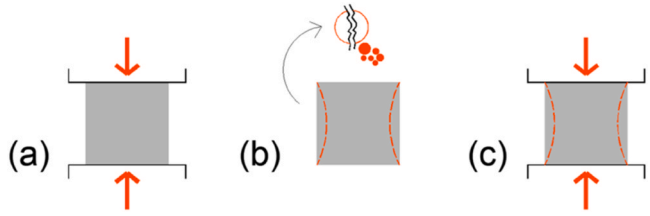

Fig. 4. Testing procedure. Stage a: pre-cracking, Stage b: healing period, Stage c: reloading after healing.

- Stage a: the samples are loaded until failure in the control tests ($\sigma_c^{0\_28}$; $\sigma_c^{0\_168}$); or until a fraction of the maximum load, such as 70 % in pre-peak regime, 90 % in pre-peak regime, 90 % in post peak regime.
- Stage b: samples are placed in laboratory environmental conditions (20° ± 5, RH ~ 45 %) for 14 days.
- Stage c: the samples are reloaded until failure ($\sigma_c^{h\_42}$; $\sigma_c^{h\_183}$);

It is important to note that healing agents are released only when the damage exceeds a certain threshold. For this reason, as shown in Fig 5, three damage levels were tested: applying 70 % of the previously measured compressive strength in the pre-peak regime, and applying 90 % in either the pre-peak or post-peak regime. As highlighted by Vonk's studies [54], in concrete under compression up to 30 % of peak stress, the increase in number and length of cracks is negligible. However, between 70 % and 90 % of peak stress, cracks begin to propagate through the mortar, and as the stress continues to increase, more cracks coalesce, leading to unstable crack growth. As a matter of fact, pre-loading samples at 90 % of the compressive strength in post-peak regime, a most significant damage is induced and a large- combined cracks which influence a much larger zone could be seen.

The experimental programme, as presented in Table 1, can be separated into 4 main groups.

The sample designation is expressed as follows: V_W_X_Y_Z where V

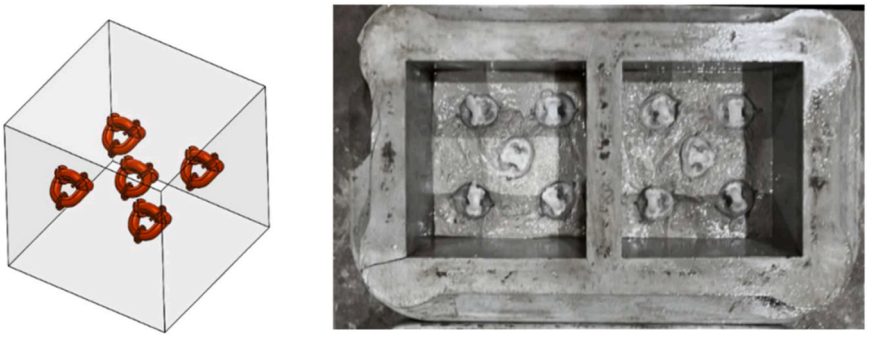

Fig 3. m-MVNs position in 100 mm side cubes (a), specimens filled to 50 mm from the base of the mould (b).

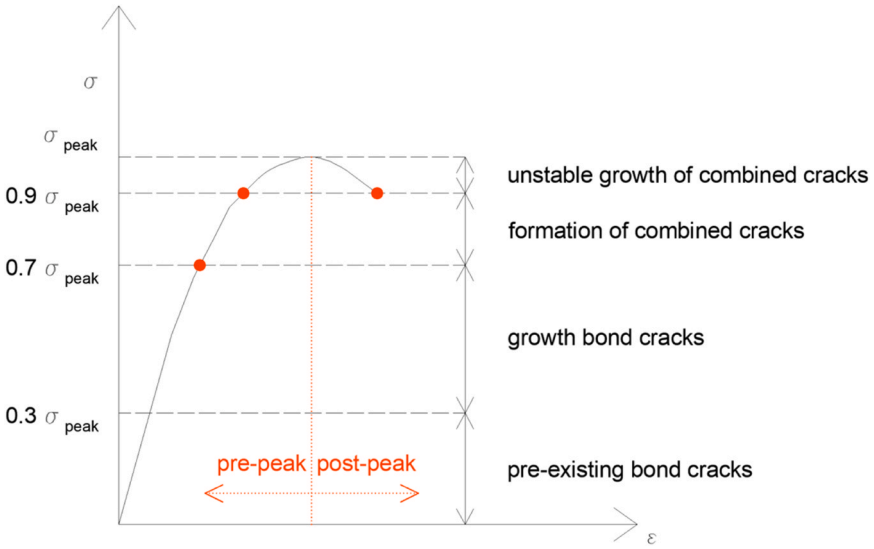

Fig. 5. Relation between the compressive stress-strain curve and crack formation.

Table 1
Experimental programme.

	Sample designation	No m-MVNs	Level of damage			Healing agents		Healing period
		5	70 % pre-peak regime	90 % pre-peak regime	90 % post-peak regime	50:50	80:20	(14 days)
GROUP_1	1_L_28	-	-	-	-	-	-	-
	1_L_28_70_pre	-	✓	-	-	-	-	✓
	1_L_28_90_pre	-	-	✓	-	-	-	✓
	1_L_28_90_post	-	-		✓	-	-	✓
	1_L_42	-	-	-	-	-	-	-
GROUP_2	2_M_28_E	✓	-	-	-	-	-	-
	2_M_28_E_70_pre	-	✓	-	-	-	-	✓
	2_M_28_E_90_pre	-	-	✓	-	-	-	✓
	2_M_28_E_90_post	-	-	-	✓	-	-	✓
	2_M_28_50:50_70_pre	✓	✓	-		✓	-	✓
	2_M_28_50:50_90_post	✓		-	✓	✓	-	✓
	2_M_28_80:20_70_pre	✓	✓			-	✓	✓
	2_M_28_80:20_90_post	✓	-	-	✓	-	✓	✓
	2_M_42_E	✓	-	-	-	-	-	-
GROUP_3	3_L_168	-	-	-	-	-	-	-
	3_L_168_70_pre	-	✓	-	-	-	-	✓
	3_L_168_90_post	-	-	-	✓	-	-	✓
	3_L_183	-	-	-	-	-	-	-
GROUP_4	4_M_168_E	-	-	-	-	-	-	-
	4_M_168_E _70_pre	✓	✓	-	-	-	-	✓
	4_M_168_E _90_pre	✓	-	✓	-	-	-	✓
	4_M_168_50:50_70_pre	✓	✓	-	-	✓	-	✓
	4_M_168_50:50_90_pre	✓	-	✓		✓	-	✓
	4_M_168_80:20_70_pre	✓	✓	-	-	-	✓	✓
	4_M_168_80:20_90_pre	✓	-	✓	-	-	✓	✓
	4_M_183_E	-	-	-	-	-	-	-

is the group number; W represents either plain lime (L) or 5 m-MVNs (M); X is the age of the first test in days; Y is the healing agent used to fill the MVNs (E = empty, no healing agents, 50:50 = 10 g/L calcium hydroxide in 50–50 % water – ethanol; 80: 20 = 10 g/L calcium hydroxide in 80–20 % water – ethanol); Z is the level of the damage (70_pre = 70 % in pre-peak regime of the compressive strength measured as above, 90_pre = 90 % of the same strength in pre-peak regime and 90_post = 90 % in post-peak regime). Three cubic specimens were cast for each sample designation.

Group_1 had two main objectives: first, to evaluate the compressive strength after 28 days, and second, to examine the impact of various damage levels on a 14-day period of autogenous healing.

A 14-day healing period was chosen, as previous studies have indicated that this timeframe is sufficient for autogenous healing to occur [34–36], allowing for a comparison with the effects of the engineered healing process activated by the m-MVNs filled with nanolime dispersions. Therefore, for comparison the strength of samples tested at 42 days (28 +14 days) was also assessed.

In Group_2, the objectives are twofold: to investigate the impact of empty m-MVNs in the lime mortar matrix, and to assess the potential of m-MVNs in delivering healing agents to damaged zones, considering the levels of damage described above. Additionally, the healing efficacy of the two tested nanolime formulations was examined.

In Group_3, the curing time was extended to 168 days to observe the effectiveness of autogenous healing at later age.

Similarly, in Group_4, the healing performance of the same nanolime formulations tested in Group_2 was evaluated in older samples at 168 days. Empty m-MVNs were also used to discern any advantages of

employing m-MVNs. For completeness the strength of samples tested at 183 days (168 +14 days) was also evaluated.

Fragments collected from crack surfaces of samples in Group_4 were also analysed with scanning electron microscopy (SEM) at Cardiff University. The latter was carried out with a Zeiss Sigma HD Field Emission Gun Analytical SEM (ASEM) equipped with an in-lens and Everhart-Thornley secondary electron detector and a backscatter electron detector.

3. Experimental results

3.1. Nanolime dispersions

Firstly, nanolimes were synthesised and dispersed in ethanol and/or water, both individually and in different combinations. The solvent mixtures with the most promising results in terms of kinetic stability were then applied to PLA samples for evaluation. The addition of water to ethanol dispersion implies the aggregation of particles and a dramatic reduction of kinetic stability.

Fig. 6 reports on the particles size distribution where Y axis refers to the number density of scattering objects. Particle size distribution measurements were carried out with a laser diffraction particle size analyzer Mastersizer 3000 equipped with a Hydro SV automatic wet dispersion unit (Malvern). Measurements were performed right after preparation of the dispersions and 24 h later. For each sample 20 repeats (acquisitions of 5 s) were performed, and an interval of 5 s was set between successive measurements

As clearly shown (Fig. 6(b)), particles agglomerate to form objects around 6–7 micron, when the water/alcohol blend reaches 50:50 V/V. With a ratio 80:20, particles size distribution moves back to lower average dimension (Fig. 6(c)), showing a broader and bimodal distribution. It can be hypothesized that such behaviour depends on the partial solubility of calcium hydroxide in the richer water mixture (80:20). Most important, re-dispersibility and viscosity of both the examined dispersions (50:50 and 80:20) did not show meaningful variations. This is essential because even when we observe a complete settling of particles inside the m-MVNs, it can be reasonably hypothesized that nanolime dispersion are able to move and diffuse through capillarity within the mortar, when m-MVNs break under application of a compressive stress.

3.2. Compression test results

For all specimens, the post-healing response was compared to the pre-cracking response to determine the healing efficacies of both compression strength and stiffness. The healing indices, assessing the influence of healing on the recovery of compressive strength and stiffness are discussed herein. The nominal compressive stress (σ_c) is obtained from the following Eq. (1), where F_n is the peak load, A is the cross section (10,000 mm^2).

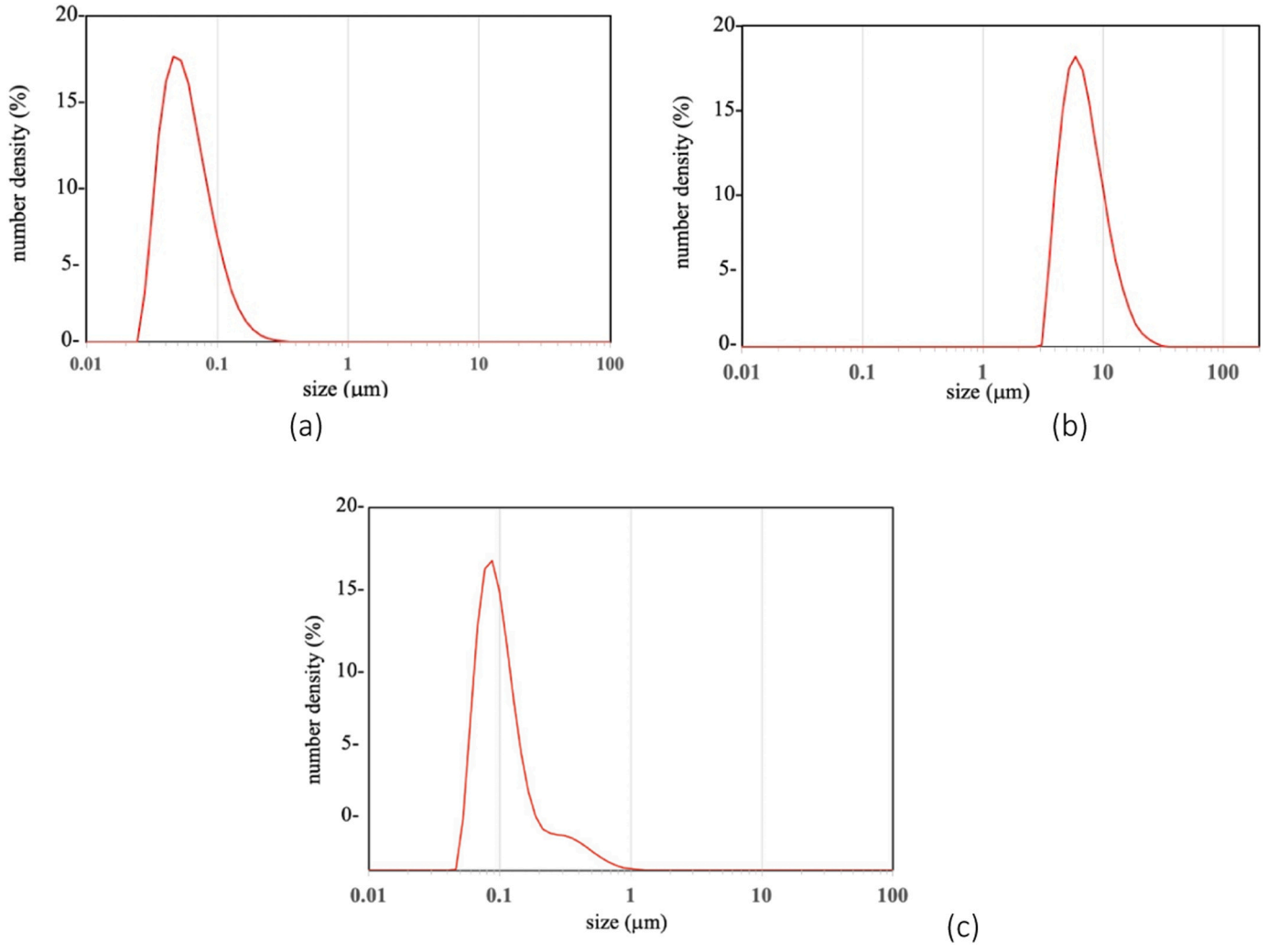

Fig. 6. Particles size distribution of lime dispersions in 100 % ethanol (a); 50:50 V/V water:ethanol blend (b); 80:20 V/V water:ethanol blend (c).

$$\sigma_c = \frac{F_n}{A} \quad (1)$$

The index of strength recovery η_σ^k (%) is defined as in equation (2), where σ_c^h is the strength gained after the healing period, σ_c^0 is the strength in undamaged condition

For the sake of clarity, indications of the age of samples were added in the superscript, for example

$\sigma_c^{0,28}$ is the maximum strength in undamaged condition evaluated at 28 days, while

$\sigma_c^{h,42}$ is the strength gained after the healing period.

Similarly, the index of stiffness recovery $\eta_E^k(\%)$ was calculated as defined in equation (3), considering E_c^h is the modulus of elasticity of the mortar after healing period, E_c^0 is the original modulus of elasticity in undamaged condition.

Index of strength recovery

$$\eta_\sigma^k(\%) = \left[\overline{\sigma}_c^h - \left(\overline{\sigma}_c^{0+14} - \overline{\sigma}_c^0\right) - \overline{\sigma}_c^0\right]/\overline{\sigma}_c^0)x100 \quad (2)$$

Index of stiffness recovery

$$\eta_E^k(\%) = \left[\overline{E}_c^h - \left(\overline{E}_c^{0+14} - \overline{E}_c^0\right) - \overline{E}_c^0\right]/\overline{E}_c^0)x100 \quad (3)$$

3.3. Group_1 results

The compression test results, along with healing indices derived from the stress-strain responses, are presented in Table 2. The data displayed in Table 2 represents the average of three specimens.

According to Lanas et al. [6] natural hydraulic lime mortar samples reveal a gradual curing process, with more significant improvement observed within the initial 28 days [6]. In fact, upon testing at 42 days of curing, there was a notable increase in both compressive strength and stiffness, with an observed enhancement of 36 % in compressive strength and an 18 % improvement in stiffness compared to the values recorded at 28 days. Therefore, evaluations of healing efficiency were conducted by comparing the results with samples tested for the first time at 42 days, as denoted in Equation 2 and 3. This allows to isolate the increase that would ordinarily occur due to natural aging from the healing response of the specimens.

It was observed that samples subjected to pre-damage at 70 % in the pre-peak regime demonstrated a slight healing index of 3 % and 14 % for strength and stiffness, respectively, confirming the influence of autogenous healing phenomena on the mechanical behaviour of natural hydraulic lime [13].

The influence of varying the extent of damage on the healing response was investigated by extending the pre-cracking phase to either 90 % in the pre-peak regime or 90 % in the post-peak regime.

With increasing levels of damage, the healing index increased by up to 9 % in the pre-peak regime, with no stiffness recovery. In the post-peak regime, no healing was observed in either strength or stiffness, with both indices showing negative values (-6 %, −18 %).

3.4. Group_2 results

The results of the compression tests conducted on natural hydraulic lime mortar containing 5 m-MVNs, either empty or filled with a 50:50 dispersion of 10 g/L calcium hydroxide in a 50–50 % water–ethanol solution (referred to as 50:50) and an 80:20 dispersion of 10 g/L calcium hydroxide in an 80–20 % water–ethanol solution (referred to as 80:20), are reported in Table 3.

As expected, compared to control specimens tested at 28 and 42 days, samples containing empty m-MVNs showed a slight reduction in compressive strength, with decreases of 22 % and 17 %, respectively. This behaviour is consistent with previous experimental observations when meso (MVNs) vascular networks were embedded in concrete matrices [32]- [33]

This difference appears to decrease to an average of 12 % when m-MVNs are filled with the selected healing agents.

No significant effect on stiffness can be observed by the presence of the m-MVNs, neither empty nor filled in undamaged phase.

In terms of healing efficacy, samples containing empty minis exhibited higher strength and stiffness recovery (+28 % and +4 %, respectively) compared to control samples pre-damaged up to 70 % in the pre-peak regime. In samples damaged up to 90 % in pre-peak regime, the presence of empty m-MVNs led to significant increases in strength and stiffness healing indices by 36 % and 9 % respectively, compared to control samples. At higher damage level, this trend is confirmed with an increase of 9 % and 16 % respectively.

It can be reasonably assumed that the inclusion of m-MVNs, even when empty, can bridge cracks in the lime mortar matrix. This potential reduction in crack width might have facilitated the filling of the cracks through the rehydration of unreacted particles (i.e., autogenous healing processes, as highlighted by [55]

Stress-strain response of samples containing m-MVNs filled with either 50:50 or 80:20 nanolime dispersions are represented in Fig. 7. Two levels of damage were considered here: the minimum and the maximum, in order to explore the system's boundary behaviour.

Regarding healing efficiency, samples containing m-MVNs filled with either 50:50 or 80:20 nanolime mixtures and pre-damaged at 70 % in the pre-peak regime exhibited a similar strength recovery of 37 %, with the 50:50 mixture showing a higher stiffness recovery of up to 71 % (57 % higher than the control and 27 % higher than the 80:20 mixture).

The healing performance observed suggests that the m-MVNs have ruptured, releasing the healing agent into the lime matrix. The volume of the healing agent was both sufficient and reactive enough, resulting in a strength regain 37 % higher than in samples containing empty m-MVNs.

Samples containing nanolimes and pre-damaged to 90 % in the post-peak regime exhibited a strength regain slightly higher to that of samples containing empty m-MVNs, yet still 12 % higher than control samples. In terms of stiffness, the highest recovery was observed in samples containing the 50:50 dispersion, with a healing index of 24 % (42 % higher than the controls), while samples containing the 80:20 dispersion showed no recovery, similar to that of empty m-MVNs.

It is worth mentioning that samples pre-cracked to 90 % of the compression strength in the post-peak regime displayed significant fragility after the cracking phase (stage b), sometimes leading to considerable loss of materials. This trend was more noticeable in control samples and marginally in samples containing m-MVNs containing the

Table 2
Group_1: compression test results and indices of healing.

Group_1	$\sigma_c^{0,28}$ MPa (CoV%)	$\sigma_c^{d,28}$ MPa (CoV%)	$\sigma_c^{0,42}$ MPa (CoV%)	$\sigma_c^{h,42}$ MPa (CoV%)	$E_c^{0,28}$ MPa (CoV%)	$E_c^{d,28}$ MPa (CoV%)	$E_c^{0,42}$ MPa (CoV%)	$E_c^{h,42}$ MPa (CoV%)	Healing $\eta_\sigma^{k,42}$ (%)	Healing $\eta_E^{k,42}$ (%)
1_L_28	3.20 (3)	-	-	-	428.9 (7)	-	-	-	-	-
1_L_28_70_pre	-	2.2 (0)	-	4.5 (5)	-	404.0(1)	-	568.2 (4)	3	14
1_L_28_90_pre	-	2.9 (2)	-	4.7 (0)	-	365.7(8)	-	510.3 (9)	9	0
1_L_28_90_post	-	2.9 (2)	-	4.2 (5)	-	264.4 (9)	-	430.2 (1)	−6	−18
1_L_42	-	-	4.4 (2)	-	-	-	508.3 (6)	-	-	-

Table 3
Group_2: compression test results and indices of healing.

Group_2	$\sigma_c^{0,28}$ MPa (CoV%)	$\sigma_c^{d,28}$ MPa (CoV%)	$\sigma_c^{0,42}$ MPa (CoV%)	$\sigma_c^{h,42}$ MPa (CoV%)	$E_c^{0,28}$ MPa (CoV%)	$E_c^{d,28}$ MPa (CoV%)	$E_c^{0,42}$ MPa (CoV%)	$E_c^{h,42}$ MPa (CoV%)	Healing $\eta_\sigma^{k,42}$ (%)	Healing $\eta_E^{k,42}$ (%)
2_M_28_E	2.5 (3)	-	-	-	448.2 (9)	-	-	-	-	-
2_M_28_E_70_pre	-	1.7 (0)	-	4.4 (5)	-	230.0 (8)	-	540.1 (16)	31	18
2_M_28_E_90_pre	-	2.3 (0)	-	4.7 (3)	-	212.7 (7)	-	502.2 (18)	45	9
2_M_28_E_90_post	-	2.3 (0)	-	3.7 (18)	-	119.5 (41)	-	449.9 (15)	3	−3
2_M_28_50:50_70_pre	-	1.7 (0)	-	4.5 (3)	-	438.2 (3)	-	780.2 (9)	37	71
2_M_28_50:50_90_post	-	2.7 (1)	-	3.7 (1)	-	100.4 (2)	-	570.9 (2)	6	24
2_M_28_80:20_70_pre	-	1.7 (0)	-	4.5 (1)	-	425.2 (0)	-	673.3 (4)	37	47
2_M_28_80:20_90_post	-	2.9 (2)	-	3.6 (4)	-	92.7 (5)	-	429.1 (9)	1	−7
2_M_42_E	-	-	3.6 (7)	-	-		461.2	-	-	-

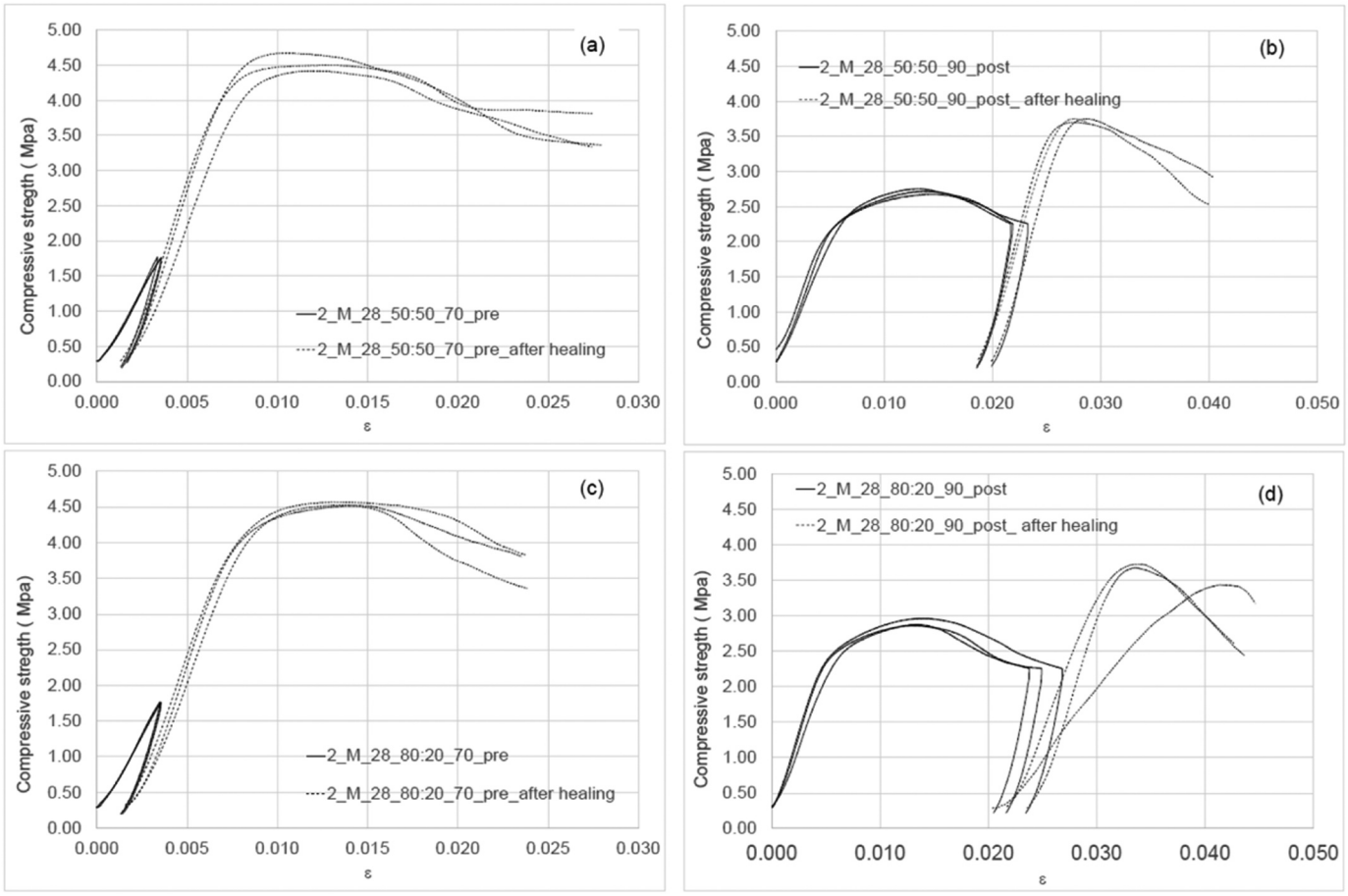

Fig. 7. Group_2 Stress strain response for samples containing m-MVNs filled with 50:50 nanolime dispersion and pre-damaged at 70 % in pre-peak regime (a); pre-damaged at 90 % in post-peak regime (b); for samples containing m-MVNs filled with 80:20 nanolime dispersion and pre-damaged at 70 % in pre-peak regime (c); pre-damaged at 90 % in post-peak regime 80:20 (d).

Table 4
Group_3: compression test results and indices of healing.

Group_3	$\sigma_c^{0,168}$ MPa (CoV%)	$\sigma_c^{d,168}$ MPa (CoV%)	$\sigma_c^{0,183}$ MPa (CoV%)	$\sigma_c^{h,183}$ MPa (CoV%)	$E_c^{0,168}$ MPa (CoV%)	$E_c^{d,168}$ MPa (CoV%)	$E_c^{0,183}$ MPa (CoV%)	$E_c^{h,183}$ MPa (CoV%)	Healing $\eta_\sigma^{k,183}$ (%)	Healing $\eta_E^{k,183}$ (%)
3_L_168	5.9 (0)	-	-	-	627 (7)	-	-	-	-	-
3_L_168_70_pre	-	4.2 (0)	-	9.32 (2)	-	638.4 (4)	-	943.0 (7)	7	37
3_L_168_90_pre	-	5.6 (0)	-	9.35 (4)	-	604.4 (9)	-	926.5 (5)	7	34
3_L_183	-	-	8.9 (4)	-	-	-	712.3 (8)	-	-	-

80:20 dispersion. Therefore, the study proceeded by solely focusing on pre-peak damages.

3.5. Group_3 results

Control samples tested to failure at either 168 or 183 days (i.e. 168 +14 days) showed compression strengths of 5.94 MPa and 8.91 MPa respectively, as reported in Table 4. Interestingly, in the later 2 weeks, the strength increased by 33 %. Regardless of the level of damage, control samples exhibited autogenous healing properties, with a similar recovery in strength (7 %). This confirms that the autogenous healing ability retains recovery potential as seen in the early stage (28 days). It also appears that with extended curing, the lime-based mortar develops an improved ability to recover stiffness, ranging from 37 % to 34 %, regardless of the level of damage.

3.6. Group_4 results

The compression test results are reported in Table 5 together with indices of healing derived from the stress-strain responses.

The inclusion of 5 empty m-MVNs placed in the center of the lime-based mortar cube yielded a performance similar to that previously observed in Group_2, with a marginal strength reduction of approximately 18 %. It was noted that in samples tested at 183 days, this reduction was mitigated to 9 %.

The presence of empty m-MVNs in samples pre-damaged either to 70 % or 90 % in the pre-peak regime seemed to promote autogenous healing performance. This resulted in a regain in strength of 20 % and 23 %, respectively (~14 % compared to control samples). In terms of stiffness, the embedding of empty m-MVNs appeared to have healing effect only at lower level of damage (+12 % with respect to control).

Stress-strain response of samples containing m-MVNs filled with either 50:50 or 80:20 nanolime dispersions are represented in Fig. 8.

Samples with m-MVNs filled with a 50:50 dispersion and pre-damaged to 70 % in the pre-peak regime demonstrated strength and stiffness recoveries of 8 % and 43 %, respectively, which were only slightly higher than those of the control samples.

Post-test observations showed that most m-MVNs remained intact, leading to limited release of healing agents. This suggests that once the lime mortar matrix has matured, 70 % pre-peak damage may be insufficient to rupture the m-MVNs. However, this does not appear to be detrimental with respect to autogenous healing phenomena and efficacy.

A similar behaviour was observed in samples containing m-MVNs filled with the 80:20 dispersion, with a slightly higher index of healing in strength (+7 % compared to 50:50 and control samples) and similar stiffness regain compared to all previously tested samples.

Samples pre-cracked at 90 % in pre-peak demonstrated the most effective healing.

Those containing m-MVNs filled with the 50:50 dispersion exhibited the best performance, with healing indices of 37 % in strength and 53 % in stiffness. Similar healing behaviour was also observed in samples containing the 80:20 dispersion, resulting in healing indices of 31 % in strength and 48 % in stiffness.

It is worth noting that when samples are pre-cracked at 90 % in pre-peak regime, the index of healing in terms of strength is in average 27 % higher than control samples and 11 % higher than in samples containing empty m-MVNS.

This indicates that the m-MVNs, a system composed of 3D-printed units filled with healing agents, are highly effective at enhancing the material's ability to heal, especially over the medium to long term, making them a valuable addition for improving the material's durability and longevity.

3.7. Morphological analysis

Self-healing effect is a direct consequence of the reactions taking place when lime comes in contact with the CO_2 entered by diffusion within mortar porosity. The presence of impurities in NHL, typically obtained by calcining argillaceous or siliceous limestones, might lead to some extent to pozzolanic reaction with lime [56], possibly contributing to the self-healing effect. A morphological analysis under electron microscope (SEM) aimed to obtain preliminary information about the reaction taking place, to support possible explanation of the self-healing process. Microstructural observations on the deposition of healing products within the lime-based matrix were performed on the crack surface adjacent to the m-MVNs.

Representative SEM images following the healing period are shown in Fig. 9.

It is well-known that the carbonation process and kinetics depend on several factors, including environmental relative humidity, type of substrate, porosity, CO_2 supply and others. Fig. 9(a) reports SEM images describing the morphology and distribution of the newly formed phase. According to López-Arce et al. findings [57]reaction of lime with CO_2 may produce needle-shaped crystals. It can be assumed that acicular crystals refer to vaterite, which typically form when reaction occurs in a humid environment. Fig. 9(b) reveals that needle-like habit aggregates of vaterite crystals (1–4 μm sized) are probably associated to round-shaped monohydrocalcite (1–2 μm sized). The direct comparison of the two images (control sample (a) and samples containing m-MVNs filled with nanolime dispersion (b)) seems suggesting the building-up of a net, growing on the pre-existing mineral phases.

Along with calcium hydroxide carbonation, another concomitant reaction could be considered. In fact, the presence of nanolime in water may initiate a pozzolanic reaction with the fine aggregate sand to produce a calcium silicate hydrate (CSH) phase, which includes a number of amorphous and poor crystalline structures with the general formula of $xCaO{\cdot}SiO_2{\cdot}yH_2O$ with varying stoichiometry. Although the analysis of the SEM images cannot provide definitive evidence of this, the crystal habitus of CSH at the early stages of hydration shows significant similarities with carbonates.

While this study does not include a quantitative assessment of the individual contributions of these two processes to the self-healing effect, which improved the mechanical properties of the treated hydraulic

Table 5
Group_4: compression test results and indices of healing.

Group_4	$\sigma_c^{0,168}$ MPa (CoV%)	$\sigma_c^{d,168}$ MPa (CoV%)	$\sigma_c^{0,183}$ MPa (CoV%)	$\sigma_c^{h,183}$ MPa (CoV%)	$E_c^{0,168}$ MPa (CoV%)	$E_c^{d,168}$ MPa (CoV%)	$E_c^{0,183}$ MPa (CoV%)	$E_c^{h,183}$ MPa (CoV%)	Healing $\eta_\sigma^{k,183}$ (%)	Healing $\eta_E^{k,183}$ (%)
4_M_168_E	4.9 (3)	-	-	-	544.0 (14)	-	-	-	-	-
4_M_168_E _70_pre	-	3.4 (0)	-	9.1 (2)	-	606.7 (7)	-	960.1 (20)	20	49
4_M_168_E _90_pre	-	4.4 (0)	-	9.2 (4)	-	515.9 (15)	-	879.3 (9)	23	35
4_M_168_50:50_70_pre	-	3.4 (0)	-	8.5 (2)	-	591.1 (6)	-	927.6 (3)	8	43
4_M_168_50:50_90_pre	-	4.4 (0)	-	9.9 (1)	-	526.5 (14)	-	980.7 (7)	37	53
4_M_168_80:20_70_pre	-	3.7 (11)	-	8.8 (0)	-	576.4 (2)	-	909.0 (3)	15	40
4_M_168_80:20_90_pre	-	4.4 (0)	-	9.3 (3)	-	571.0 (11)	-	950.4 (3)	31	48
4_M_183_E	-	-	8.1(11)	-	-	-	691.0 (11)	-	-	-

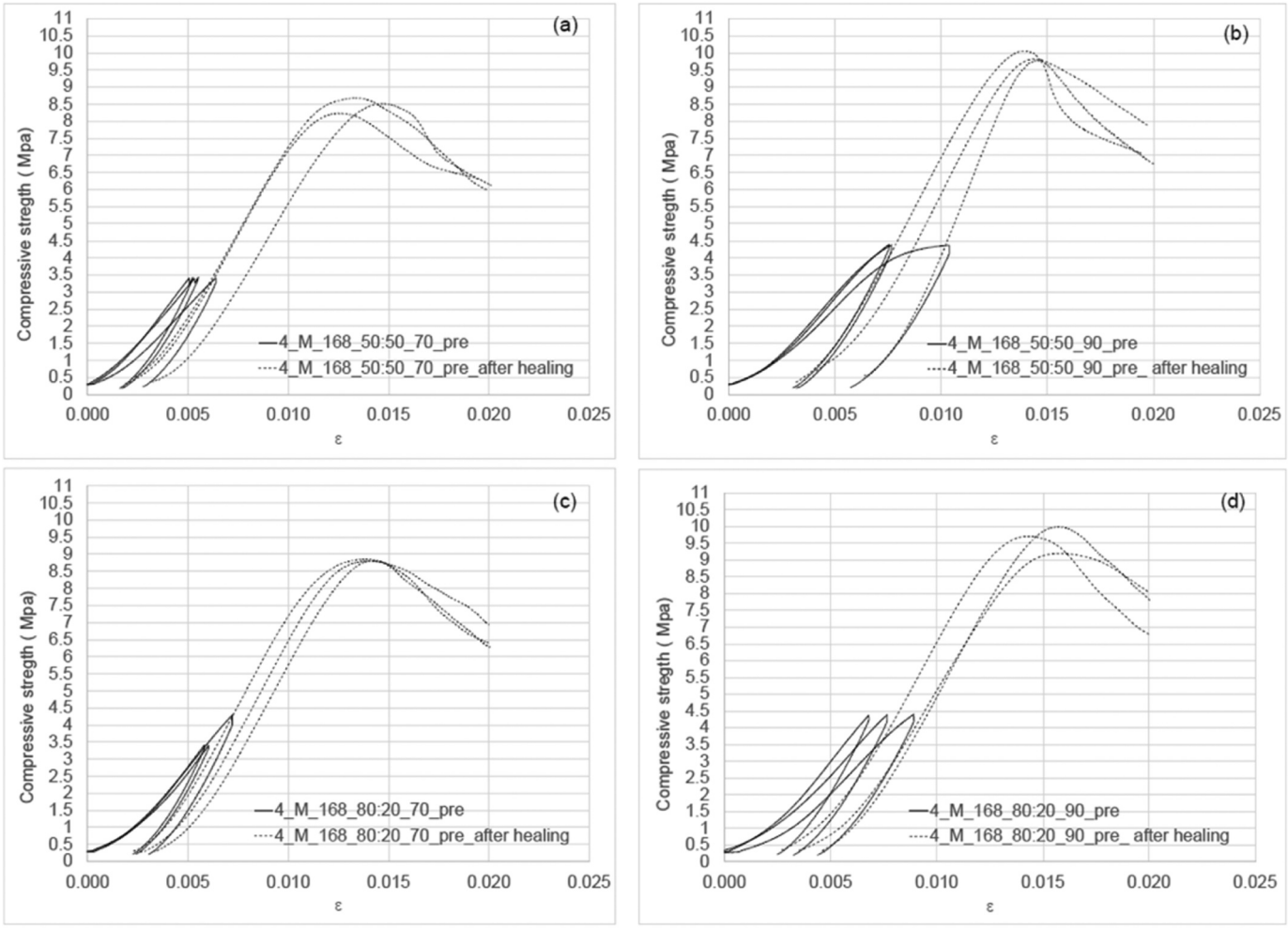

Fig. 8. Group_4: stress strain response for samples containing m-MVNs filled with 50:50 nanolime dispersion and pre-damaged at 70 % in pre-peak regime (a); pre-damaged at 90 % in pre-peak regime (b); for samples containing m-MVNs filled with 80:20 nanolime dispersion and pre-damaged at 70 % in pre-peak regime, sample 3 was unintentionally pre-damaged to a level of 4.3 MPa (c); pre-damaged at 90 % in pre-peak regime 80:20 (d).

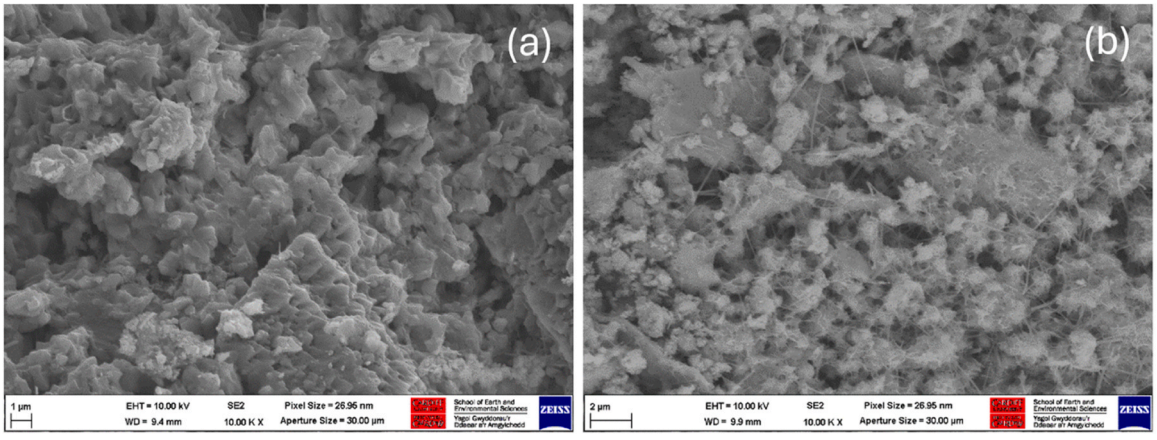

Fig. 9. SEM images from the fracture surface of control sample (a) and samples containing m-MVNs filled with 50:50 dispersion.

mortar, this remains a crucial next step for fully understanding the potential of this approach. This research establishes a solid foundation for future studies to further investigate and quantify these mechanisms.

4. Prospects and limitations

m-MVNs represent an innovative and flexible self-healing technology for lime-based mortars, offering a sustainable and effective solution to enhance the durability and resilience of historic masonry structures. By integrating biomimetic 4D-printed m-MVNs into patching techniques,

this approach addresses the preservation needs of built heritage while promoting longevity and compatibility with traditional materials. The system is adaptable, allowing minor geometric adjustments to fit localised joints while effectively delivering tailored healing agents for long-term durability.

However, challenges remain, including ensuring the consistent rupture of m-MVNs under damage conditions, optimising healing agent formulations for diverse environmental scenarios, and addressing potential interactions between the healing agents and the host materials.

Further research is needed to fully quantify the contributions of different healing mechanisms, explore the potential for cyclic healing to address recurring damage, and enhance scalability for widespread application in conservation practices.

5. Conclusion

This paper presents an innovative biomimetic self-healing technology based on mortar mini-vascular networks (m-MVNs), which can be embedded in mortar joints during patching techniques to restore historic masonry structures. The m-MVNs consist of 4D-printed hollow units that act as reservoirs for healing agents, remaining dormant until activated and released when damage exceeds a specific threshold.

To study effective and compatible healing agents for historic materials, two nanolime blends with varying alcohol/water ratios were evaluated, i.e. 10 g/L of calcium hydroxide in either a 50:50 % (referred as 50:50) or 80–20 % water–ethanol (referred as 80:20) dispersion.

Five m-MVNs, either empty or filled with nanolime dispersions in 50:50 or 80:20 ratios, were embedded in the center of 100 mm cubic hydraulic lime mortar samples. The samples were pre-cracked at different ages (28–196 days) and levels of damage (70 % of compression strength in the pre-peak regime; 90 % in both the pre- and post-peak regimes) and then allowed to heal for 14 days in laboratory environment.

From the analyses of the results presented in the paper, the following main conclusions can be drawn:

- natural hydraulic lime mortar samples (referred as control) confirmed autogenous healing ability which appeared to significantly decrease with the increase level of damage but not with the age of sample. The ceiling values for strength and stiffness recovery were found to be in a range of 3–7 % and 34–37 % respectively.
- the presence of empty m-MVNs had a slight effect on strength but did not impact stiffness in undamaged samples, with strength decreasing from 22 % at 28 days to 9 % at 168 days. Following damage, empty m-MVNs appear to enhance autogenous healing, potentially aiding in bridging cracks within the lime mortar matrix, reducing crack width, and promoting effective filling through autogenous healing processes.
- at 28 days, samples containing m-MVNs filled with either 50:50 or 80:20 nanolime dispersions and pre-damaged at 70 % in the pre-peak regime showed a significant and similar regain in strength up to 37 %. 50:50 dispersion appeared to enhance healing in terms of stiffness, achieving up to 71 % recovery, which was 57 % higher than the control and 27 % higher than samples containing m-MVNs filled with 80:20 nanolime. Samples pre-damaged up to 90 % in the post-peak regime still demonstrated positive recovery in strength (up to 6 %) and stiffness (up to 24 %), despite exhibiting significant fragility after the cracking phase.
- at later stage (i.e. at 168 days), pre-damage at 70 % in the pre-peak regime was insufficient to rupture the m-MVNs and release the healing agents. Post-test observations confirmed that most m-MVNs remained intact, with both nanolime dispersions still stored in liquid form. It is worth noting that this did not adversely affect the autogenous healing process, as the healing indices for both strength and stiffness were maintained or increased (+6 % in 50:50 samples). Interesting healing behaviours have been observed in samples pre-damaged up to 90 % in post-peak regime, with ceiling value of 37 % and 53 % in strength and stiffness respectively is samples containing 50:50 nanolime dispersions.

In summary, while the presence of empty m-MVNs does not significantly alter the mechanical behaviour of natural hydraulic lime, whether undamaged or damaged, they do contribute to enhancing autogenous healing. The 50:50 dispersion, showed the most promising healing results over time. The alcohol-to-water ratio also did not significantly affect the properties of the PLA polymer, enabling effective rupture during damage and successful release of the nanolime dispersion. The healing results indicated that the nanolime volume was sufficient and its reactivity with the lime matrix effectively facilitated the healing processes.

CRediT authorship contribution statement

Cristina De Nardi: Writing – review & editing, Writing – original draft, Validation, Supervision, Resources, Project administration, Methodology, Investigation, Funding acquisition, Formal analysis, Data curation, Conceptualization. **Rodorico Giorgi:** Writing – review & editing, Methodology.

Declaration of Competing Interest

The authors declare that there is no conflict of interests regarding the publication of the paper.

Acknowledgements

Cristina De Nardi reported that the research was funded by the Leverhulme Trust ECF-2022–235.

The authors would like to thank Dr. Diane Gardner for her support.

The authors also acknowledge the considerable help and expertise of Richard Thomas, Ian King, Carl Wadsworth, Samuel Moeller, Andrea Casini, Teresa Guaragnone and PAP without whom the laboratory work would not have been possible.

Data availability

Data will be made available on request.

References

[1] L. Fusade, H.A. Viles, A comparison of standard and realistic curing conditions of natural hydraulic lime repointing mortar for damp masonry: impact on laboratory evaluation, J. Cult. Herit. 37 (2019) 82–93, https://doi.org/10.1016/j.culher.2018.11.011.

[2] R. Van Hees, K. van Balen, B. Bicer-Simsir, L. Binda, T. von Konow, J.E. Lindqvist, P. Maurenbrecher, I. Papayanni, M. Subercaseaux, C. Tedeschi, E.E. Toumbakari, M. Thompson, J. Valek, R. Veiga, RILEM TC 203-RHM: Repair mortars for historic masonry: repair mortars for historic masonry. from problem to intervention: a decision process, Mater. Struct. /Mater. Et. Constr. 45 (2012) 1295–1302, https://doi.org/10.1617/s11527-012-9917-z.

[3] C. Groot, R. Veiga, I. Papayianni, R. Van Hees, M. Secco, J.I. Alvarez, P. Faria, M. Stefanidou, RILEM TC 277-LHS Report: Lime-based Mortars for Restoration–a Review on Long-term Durability Aspects and Experience from Practice, 2022. https://doi.org/10.1617/s11527-022-02052-1.

[4] A. A., C. G, The influence of aggregate texture, morphology and grading on the carbonation of non-hydraulic (aerial) lime-based mortars, Q. J. Eng. Geol. Hydrogeol. 46 (2013) 507–520, https://doi.org/10.1144/qjegh2012-017.

[5] C. Parra-Fernández, A. Arizzi, M. Secco, G. Cultrone, The manufacture of natural hydraulic limes: influence of raw materials' composition, calcination and slaking in the crystal-chemical properties of binders, Cem. Concr. Res. 185 (2024), https://doi.org/10.1016/j.cemconres.2024.107631.

[6] J. Lanas, R. Sirera, J.I. Alvarez, Study of the mechanical behavior of masonry repair lime-based mortars cured and exposed under different conditions, Cem. Concr. Res. 36 (2006) 961–970, https://doi.org/10.1016/j.cemconres.2005.12.003.

[7] F.O. Anderegg, Autogeneous healing in mortars containing lime, AST M Bullentin 22 (1942).

[8] B. Lubelli, T.G. Nijland, R.P.J. Van Hees, Self-healing of lime based mortars: microscopy observations on case studies, Heron 56 (2011).

[9] R. Fort, D. Ergenç, N. Aly, M. Alvarez de Buergo, S. Hemeda, Implications of new mineral phases in the isotopic composition of Roman lime mortars at the Kom el-Dikka archaeological site in Egypt, Constr. Build. Mater. 268 (2021) 121085, https://doi.org/10.1016/j.conbuildmat.2020.121085.
[10] C. De Nardi, S. Sayadi, I. Mihai, A. Jefferson, Simulation of Autogenous Self-Healing in Lime-Based Mortars, Int J. Numer. Anal. Methods Geomech. (2024), https://doi.org/10.1002/nag.3870.
[11] F. Grosso Giordano, M. Brunin, N. Boon, N. De Belie, On the use of non-destructive testing for the measurement of self-healing in lime-based mortars, Mater. Today Proc. (2023), https://doi.org/10.1016/j.matpr.2023.07.367.
[12] L. Garijo, J.J. Ortega, G. Ruiz, De La Rosa, X.X. Zhang, Effect of loading frequency on the fatigue life in compression of natural hydraulic lime mortars, Theor. Appl. Fract. Mech. 118 (2022) 103201, https://doi.org/10.1016/j.tafmec.2021.103201.
[13] C. De Nardi, A. Cecchi, L. Ferrara, A. Benedetti, D. Cristofori, Effect of age and level of damage on the autogenous healing of lime mortars, Compos B Eng. 124 (2017) 144–157, https://doi.org/10.1016/j.compositesb.2017.05.041.
[14] C. De Nardi, S. Bullo, L. Ferrara, L. Ronchin, A. Vavasori, Effectiveness of crystalline admixtures and lime/cement coated granules in engineered self-healing capacity of lime mortars, Mater. Struct. /Mater. Et. Constr. 50 (2017), https://doi.org/10.1617/s11527-017-1053-3.
[15] D. Ergenç, A. Sierra-Fernandez, M. del M. Barbero-Barrera, L.S. Gomez-Villalba, R. Fort, Assessment on the performances of air lime-ceramic mortars with nano-Ca(OH)2 and nano-SiO2 additions, Constr. Build. Mater. 232 (2020) 117163, https://doi.org/10.1016/j.conbuildmat.2019.117163.
[16] K. Santhanam, R. Ramadoss, Sustainability development and performance evaluation of natural hydraulic lime mortar for restoration, Environ. Sci. Pollut. Res. 29 (2022) 79634–79648, https://doi.org/10.1007/s11356-022-21019-x.
[17] S. Vucetic, B. Miljevic, O. Sovljanski, J.M. van der Bergh, S. Markov, H. Hirsenberger, M. Tzoutzouli Malesevic, J. Ranogajec, Functional mortars for conservation of cultural heritage structures, IOP Conf. Ser. Mater. Sci. Eng. 949 (2020), https://doi.org/10.1088/1757-899X/949/1/012091.
[18] S. Vučetić, D. Čjepa, B. Miljević, J.M. van der Bergh, O. Šovljanski, A. Tomić, E. Nikolić, S. Markov, H. Hiršenberger, J. Ranogajec, Bio-stimulated surface healing of historical and compatible conservation mortars, Materials 16 (2023), https://doi.org/10.3390/ma16020642.
[19] E. Tsangouri, A decade of research on self-healing concrete, in: S. Hemeda (Ed.), Sustainable Construction and Building Materials, IntechOpen, Rijeka, 2018, https://doi.org/10.5772/intechopen.82525.
[20] C. Dry, Design of Self-growing, Self-sensing and Self-repairing Materials for Engineering Applications 4234 (2001) 23–29.
[21] C. Dry, Development of a Self Repairing Durable Concrete The Problem: Damage in Concrete, Repair Efficacy and Cost the Solution: Self Repair: the Answer to Damage in Concrete, (n.d.) 1–14.
[22] K. Van Tittelboom, N. De Belie, D. Van Loo, P. Jacobs, Self-healing efficiency of cementitious materials containing tubular capsules filled with healing agent, Cem. Concr. Compos 33 (2011) 497–505, https://doi.org/10.1016/j.cemconcomp.2011.01.004.
[23] A. Pelletier, M. Brown, R. Shukla, A. Bose, Self-healing Concrete with A Microencapsulated Healing Agent (2011).
[24] E. Tsangouri, J. Lelon, P. Minnebo, H. Asaue, T. Shiotani, K. Van Tittelboom, N. De Belie, D.G. Aggelis, D. Van Hemelrijck, Feasibility study on real-scale, self-healing concrete slab by developing a smart capsules network and assessed by a plethora of advanced monitoring techniques, Constr. Build. Mater. 228 (2019) 116780, https://doi.org/10.1016/j.conbuildmat.2019.116780.
[25] Y. Shields, E. Tsangouri, C. Riordan, C. De Nardi, J.R.A. Godinho, P. Antonaci, D. Palmer, A. Al-Tabbaa, T. Jefferson, N. De Belie, K. Van Tittelboom, Non-destructive evaluation of ductile-porous versus brittle 3D printed vascular networks in self-healing concrete, Cem. Concr. Compos 145 (2024), https://doi.org/10.1016/j.cemconcomp.2023.105333.
[26] A. Formia, S. Terranova, P. Antonaci, N.M. Pugno, J.M. Tulliani, Setup of Extruded Cementitious Hollow Tubes as Containing/Releasing Devices in Self-Healing Systems, (2015) 1897–1923. https://doi.org/10.3390/ma8041897.
[27] P. Minnebo, G. Thierens, G. De Valck, K. Van Tittelboom, N. De Belie, D. Van Hemelrijck, E. Tsangouri, A novel design of autonomously healed concrete: towards a vascular healing network, Materials 10 (2017) 1–23, https://doi.org/10.3390/ma10010049.
[28] L. Ferrara, V. Krelani, Engineering self healing capacity of cement based materials through crystalline admixtures, in: Proceedings of the ICSHM2015 International Conference on Self-Healing Materials, Durham, NC (U.S.A.) (2015) 1–4.
[29] D. Snoeck, K. Van Tittelboom, S. Steuperaert, P. Dubruel, N. De Belie, Self-healing cementitious materials by the combination of microfibres and superabsorbent polymers, J. Intell. Mater. Syst. Struct. 25 (2014) 13–24, https://doi.org/10.1177/1045389X12438623.
[30] K. Van Tittelboom, J. Wang, M. Araújo, D. Snoeck, E. Gruyaert, B. Debbaut, H. Derluyn, V. Cnudde, E. Tsangouri, D. Van Hemelrijck, N. De Belie, Comparison of different approaches for self-healing concrete in a large-scale lab test, Constr. Build. Mater. 107 (2016) 125–137, https://doi.org/10.1016/j.conbuildmat.2015.12.186.
[31] D. Snoeck, N. Roigé, S. Manso, I. Segura, N. De Belie, The effect of (and the potential of recycled) superabsorbent polymers on the water retention capability and bio-receptivity of cementitious materials, Resour. Conserv Recycl 177 (2022) 106016, https://doi.org/10.1016/j.resconrec.2021.106016.
[32] C. De Nardi, D. Gardner, A.D. Jefferson, Development of 3D printed networks in self-healing concrete, Materials 13 (2020) 1328, https://doi.org/10.3390/ma13061328.
[33] C.De Nardi, D. Gardner, D. Cristofori, L. Ronchin, A. Vavasori, T, Jefferson, Advanced 3D printed mini-vascular network for self-healing concrete, Mater. Des. 230 (2023), https://doi.org/10.1016/j.matdes.2023.111939.
[34] M.R. Valluzzi, F. Casarin, E. Garbin, F. Da Porto, C. Modena, Long-term damage on masonry towers case studies and intervention strategies, in: Proceedings of the Eleventh International Conference on Fracture 2005, ICF11 (2005) 3253–3256.
[35] C. Modena, M.R. Valluzzi, F. Da Porto, F. Casarin, Structural aspects of the conservation of historic masonry constructions in seismic areas: remedial measures and emergency actions, Int. J. Archit. Herit. 5 (2011) 539–558, https://doi.org/10.1080/15583058.2011.569632.
[36] Nanolime A. Practical Guide to its Use for Consolidating Weathered Limestone << Contents, n.d.
[37] V. Daniele, G. Taglieri, R. Quaresima, The nanolimes in Cultural Heritage conservation: characterisation and analysis of the carbonatation process, J. Cult. Herit. 9 (2008) 294–301, https://doi.org/10.1016/j.culher.2007.10.007.
[38] D, G.R. Baglioni Piero, Chelazzi, Innovative nanomaterials: principles, availability and scopes, in: Nanotechnologies in the Conservation of Cultural Heritage: A Compendium of Materials and Techniques, Springer Netherlands, Dordrecht, 2015, pp. 1–14, https://doi.org/10.1007/978-94-017-9303-2_1.
[39] R. Giorgi, L. Dei, P. Baglioni, A new method for consolidating wall paintings based on dispersions of lime in alcohol, Stud. Conserv. 45 (2000) 154–161, https://doi.org/10.1179/sic.2000.45.3.154.
[40] M. Ambrosi, L. Dei, R. Giorgi, C. Neto, P. Baglioni, Colloidal particles of Ca(OH)2: properties and applications to restoration of frescoes, Langmuir 17 (2001) 4251–4255, https://doi.org/10.1021/la010269b.
[41] J. Otero, V. Starinieri, A.E. Charola, Nanolime for the consolidation of lime mortars: a comparison of three available products, Constr. Build. Mater. 181 (2018) 394–407, https://doi.org/10.1016/j.conbuildmat.2018.06.055.
[42] G. Poggi, N. Toccafondi, D. Chelazzi, P. Canton, R. Giorgi, P. Baglioni, Calcium hydroxide nanoparticles from solvothermal reaction for the deacidification of degraded waterlogged wood, J. Colloid Interface Sci. 473 (2016) 1–8, https://doi.org/10.1016/j.jcis.2016.03.038.
[43] A. Campbell, A. Hamilton, T. Stratford, S. Modestou, I. Ioannou, Calcium hydroxide nanoparticles for limestone conservation: imbibition and adhesion, Mercury (2011) 1–16.
[44] C. Rodriguez-Navarro, E. Ruiz-Agudo, Nanolimes: From synthesis to application, Pure Appl. Chem. 90 (2018) 523–550, https://doi.org/10.1515/pac-2017-0506.
[45] R. Camerini, G. Poggi, D. Chelazzi, F. Ridi, R. Giorgi, P. Baglioni, The carbonation kinetics of calcium hydroxide nanoparticles: a boundary nucleation and growth description, J. Colloid Interface Sci. 547 (2019) 370–381, https://doi.org/10.1016/j.jcis.2019.03.089.
[46] E. Spezi, M. Bray, in: Proceedings of the Cardiff University Engineering Research Conference 2023, in: n.d. https://doi.org/10.18573/conf1.
[47] J. Otero, A.E. Charola, C.A. Grissom, V. Starinieri, An Overview of Nanolime as A Consolidation Method for Calcareous Substrates, Ge-Conservacion 1 (2017) 71–78.
[48] G. Borsoi, B. Lubelli, R. van Hees, R. Veiga, A.S. Silva, Optimization of nanolime solvent for the consolidation of coarse porous limestone, Appl. Phys. A Mater. Sci. Process 122 (2016), https://doi.org/10.1007/s00339-016-0382-3.
[49] BS EN 459-1. Building lime, Definitions,Specifications and Conformity Criteria., British Standards Institution, London (2015).
[50] British Standard, BS EN 13139:2013 - Aggregates for Mortar, (2013).
[51] A. Moropoulou, A.S. Cakmak, G. Biscontin, A. Bakolas, E. Zendri, Advanced Byzantine cement based composites resisting earthquake stresses: the crushed brick/lime mortars of Justinian's Hagia Sophia, Constr. Build. Mater. 16 (2002) 543–552, https://doi.org/10.1016/S0950-0618(02)00005-3.
[52] D. Marastoni, A. Benedetti, L. Pelà, G. Pignagnoli, Torque Penetrometric Test for the in-situ characterisation of historical mortars: fracture mechanics interpretation and experimental validation, Constr. Build. Mater. 157 (2017) 509–520, https://doi.org/10.1016/j.conbuildmat.2017.09.120.
[53] L. Garijo, X. Zhang, G. Ruiz, J.J. Ortega, Age effect on the mechanical properties of natural hydraulic and aerial lime mortars, Constr. Build. Mater. 236 (2020), https://doi.org/10.1016/j.conbuildmat.2019.117573.
[54] Rene Vonk, Softening of Concrete Loaded in Compression, Technische Universiteit Eindhoven (1992), https://doi.org/10.6100/IR375705.
[55] L. Garijo, Á. De La Rosa, R. Gonzalo, O.J. Joaquín, Autogenous self-healing induced by compressive fatigue in hydraulic lime mortars, Und Rev. (2023).
[56] A. Smith, NaturaL Hydraulic Limes Limestone 2 (2005).
[57] P. López-Arce, L.S. Gomez-Villalba, L. Pinho, M.E. Fernández-Valle, M.Á. de Buergo, R. Fort, Influence of porosity and relative humidity on consolidation of dolostone with calcium hydroxide nanoparticles: effectiveness assessment with non-destructive techniques, Mater. Charact. 61 (2010) 168–184, https://doi.org/10.1016/j.matchar.2009.11.007.